Journal of Materials Chemistry C

COMMUNICATION

View Article Online
View Journal | View Issue

Cite this: J. Mater. Chem. C, 2017, 5, 8027

Received 2nd June 2017,
Accepted 21st July 2017

DOI: 10.1039/c7tc02428b

rsc.li/materials-c

Flexible and stretchable mechanoluminescent fiber and fabric†

Jing Zhang,‡ Luke Bao,‡ Huiqing Lou, Jue Deng, Ao Chen, Yajie Hu, Zhitao Zhang, Xuemei Sun * and Huisheng Peng *

With the rapid development of wearable devices, rigid and structurally inelastic conventional luminescent devices with heavy energy supply systems can hardly meet the requirements for flexibility and stretchability. Herein, we created a highly stretchable and flexible mechanoluminescent fiber based on transition metal-doped zinc particles and poly(dimethylsiloxane) by a feasible coating method. The resulting composite fiber emitted an intensity-tunable soft light upon stretching and releasing. Moreover, the structure and optical performance were well retained even after 10 000 cycles of stretching and releasing. Furthermore, the color of the composite fiber could also be tuned as green, yellow or orange, and these colors could even be combined in a single fiber. Finally, mechanoluminescent fabrics with various displays were also fabricated by a similar strategy.

In the past decade, the emergence of wearable devices has promoted the development of a variety of fields such as displaying technologies, sensing, electronics, and energy harvesting and storage.[1–6] Luminescent devices, as a representative display unit, are urgently required to be flexible and wearable.[7–13] However, conventional luminescent devices typically based on planar and bulky structures with heavy energy supply systems can hardly meet the requirements of next-generation wearable devices due to their poor breathability, flexibility and integrability.[14–17] Fibers, as the basic unit of a fabric, can be feasibly incorporated into breathable fabrics, and this may provide a promising strategy for the fabrication of wearable devices.[18–23] However, reports on fiber-shaped luminescent devices are scarce.[24] Previously, we developed some fiber-shaped polymeric light-emitting electrochemical cells.[25,26] However, their complex multilayered structures required rigorous fabrication processes, which made it difficult to realize various displays.[25,27] Based on an inelastic metal substrate, their flexibility was poor and easily broke during bending. Considering that stretchability is a basic and crucial property to mimic the variety of irregular movements of the human body, it is of great significance to find flexible as well as stretchable one-dimensional luminescent devices.

On the other hand, almost all luminescent devices rely heavily on an energy supply system which sacrifices the wearing comfort and lightweight property. Therefore, luminescent materials able to generate light under manual stimuli, such as mechanical deformation, have attracted an increasing deal of interest.[28–31] Mechanoluminescent devices, which emit reproducible light upon deformation such as stretching, can fully utilize the kinetic energy generated during our movements, making them particularly suitable for wearable devices. Furthermore, mechanoluminescent devices with simple components and structures not only are easy to fabricate, but also exhibit a highly stable mechanical and optical performance.[32] Although some mechanoluminescent ZnS:Mn particle-based fibers or fabric-like matrix devices that could monitor *in situ* damage have been reported,[33,34] these were unsuitable for flexible displays or wearable devices due to their lack of flexibility and stretchability. Finally, to the best of our knowledge, there are no reports on stretchable mechanoluminescent fibers and fabrics for flexible displays.

In this Communication, a stretchable and flexible mechanoluminescent fiber was created by simply depositing a mechanoluminescent transition metal-doped zinc sulfide (ZnS)/polydimethylsiloxane (PDMS)-based material onto an elastic fiber. This mechanoluminescent fiber emitted a reproducible and soft light upon stretch and release, and its mechanoluminescence intensity and color could be tuned by controlling the composition and structure of the composite fiber or by varying the applied mechanical force. In addition, a single fiber can emit multicolored light to satisfy the demands of a range of displays. The mechanoluminescent fiber was stable in the mechanical and optical performance after deformation activities such as stretching, twisting and bending for over 10 000 cycles. These fibers were subsequently woven into fabrics for stretchable and flexible displays and night illumination devices.

State Key Laboratory of Molecular Engineering of Polymers, State Key Laboratory of Molecular Engineering of Polymers, Department of Macromolecular Science, and Laboratory of Advanced Materials, Fudan University, Shanghai, 200438, China. E-mail: sunxm@fudan.edu.cn, penghs@fudan.edu.cn

† Electronic supplementary information (ESI) available. See DOI: 10.1039/c7tc02428b

‡ These authors contributed equally to this work.

The mechanoluminescent fiber was fabricated by sequentially depositing ZnS:Cu/PDMS and PDMS layers onto a PDMS fiber (Fig. 1a and ESI†). The ZnS:Cu particles had an average diameter of 28 μm (Fig. S1, ESI†) and ZnS exhibited the zinc blende crystal phase (Fig. S2, ESI†). After being coated, the PDMS fiber was uniformly surrounded by the mechanoluminescent ZnS:Cu/PDMS material (Fig. 1b), in which the ZnS:Cu particles were well distributed within the PDMS matrix (Fig. 1c). The final composite fiber showed a clear core–sheath structure composed of an inner PDMS fiber, a mechanoluminescent ZnS:Cu/PDMS interlayer with a thickness of approximately 200 μm and an outer PDMS sheath (Fig. 1d and e). The elemental mapping images in Fig. 1f–h demonstrate that PDMS, containing silicon, held the entire core–sheath structure together, while the ZnS:Cu particles were uniformly embedded within it. The high content and full connection of PDMS enabled the composite fiber to be flexible and stable, and the structure was maintained well even after 10 000 cycles of stretching and releasing (Fig. S3, ESI†).

The resulting composite fiber could emit green light upon stretch and release (Fig. S4 and Video, ESI†). Generally, mechanoluminescence is conventionally produced by stress-induced luminescence mechanism,[35,36] and a triboelectricity-induced luminescence mechanism was also recently proposed,[37,38] which is yet to be validated. To investigate the mechanoluminescence in this composite fiber, we designed a stretch-release system able to provide a periodic stress for a systematic study (Fig. S5 and ESI†).

Firstly, the content of ZnS:Cu phosphor particles showed a significant effect on the luminescence intensity. As shown in Fig. 2a, the mechanoluminescence intensity of the ZnS:Cu/PDMS fiber linearly increased from 0.89 to 9.04 cd m^{-2} as the content of ZnS:Cu particles increased from 20% to 70%. Although the mechanoluminescence intensity increased by nearly tenfold, the breaking strength showed a dramatic decrease from 6.26 to 1.88 MPa (Fig. S6, ESI†). Based on these results, a composite fiber with a unique core–sheath structure was developed. The inner PDMS fiber not only remarkably enhanced the breaking strength to 4.61 MPa, even at a high ZnS:Cu content of 70% in the active layer (Fig. S7, ESI†), but also increased the breaking elongation from 116.9% to 175.4%. In addition, the mechanoluminescence intensity of the composite fiber also depended on the thickness of the mechanoluminescent ZnS:Cu/PDMS interlayer. Thus, the mechanoluminescence intensity linearly increased from 1.66 to 15.14 cd m^{-2} as the thickness of the interlayer increased from 140 to 680 μm (Fig. 2b).

In addition to the thickness of the mechanoluminescent interlayer, the applied mechanical force including strain and frequency also affected the intensity. As the strain increased from 45% to 70%, initially, the mechanoluminescence intensity of the composite fiber rapidly rose from 3.41 to 7.51 cd m^{-2}, and then slowly increased to 8.55 cd m^{-2} at a higher strain of 120% (Fig. 2c). This was consistent with the stress–strain curve of the mechanoluminescent fiber (Fig. S7, ESI†). At a low strain below 70%, it was easier for the mechanoluminescent fiber to undergo a large deformation upon a small stress increase, indicating that a larger relative movement between the ZnS particles and the PDMS matrix occurred easily. This suggested that the mechanism for mechanoluminescence in the composite fiber is more likely to be triboelectricity-induced, rather

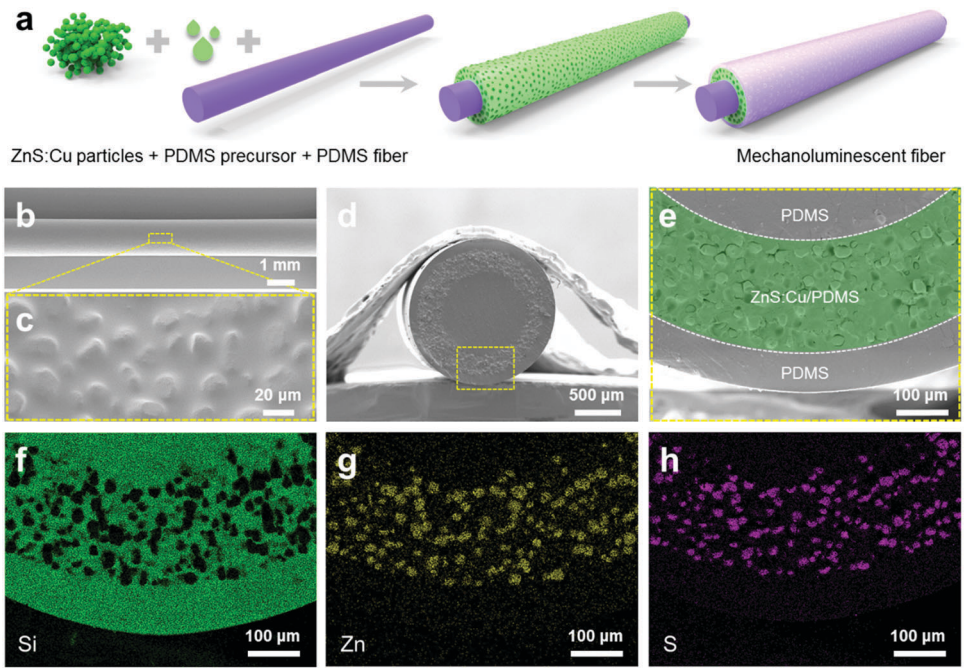

Fig. 1 Structural characterization of the mechanoluminescent fiber. (a) Schematic illustration for the preparation of the mechanoluminescent composite fiber; (b) and (c) side view of the mechanoluminescent fiber without the outer PDMS layer at low and high magnifications, respectively; (d) and (e) cross-sectional view of the mechanoluminescent fiber at low and high magnifications, respectively; (f–h) energy dispersive spectroscopy mapping images of (e) for silicon, zinc and sulfur, respectively.

than stress-induced. Therefore, at a higher strain (70% to 120%), the mechanoluminescence intensity increased slowly because the fiber became stiff and there was not sufficient soft friction between the ZnS particles and the PDMS matrix. The mechanoluminescence intensity generated by the composite fiber at increasing stretch frequencies from 2 to 8 Hz is shown in Fig. 2d. The mechanoluminescence intensity increased according to a linear relationship from 3.60 to 10.35 cd m^{-2}, as more lights could be detected with a spectroradiometer in the same measurement time.[32]

The mechanoluminescent fiber showed a highly reversible light-emitting property. As shown in Fig. 2e, the mechanoluminescence intensity of the composite fiber dramatically decreased in the first 1000 cycles (3 min) from 10.75 to 5.32 cd m^{-2}, which was nearly ~50% of the initial intensity. Thereafter, the mechanoluminescence intensity stabilized and was retained by 81.2% (4.32 cd m^{-2}) after further 9000 cycles (30 min) of stretch and release. The degradation of the mechanoluminescence intensity in the composite fiber was caused either by decay of the ZnS:Cu phosphor or fatigue of the PDMS matrix.

To determine the factors that led to degradation of the mechanoluminescence intensity, we firstly compared the non-stretched region (both ends of the fiber) with the stretched region (middle part of the fiber) of the same composite fiber in the corresponding photoluminescent image (inset of Fig. 2e). No obvious luminescence difference was observed between the two regions, suggesting that the properties of the ZnS:Cu phosphor were largely retained. Then, the properties of the PDMS matrix were investigated by measuring its tensile stress during deformation tests. During the stretch and release process at a constant strain, the stress of the mechanoluminescent composite fiber remarkably decreased within the first 3 minutes from 5.07 to 4.51 MPa, and subsequently remained at about 4.35 MPa. The variation trend in tensile stress was

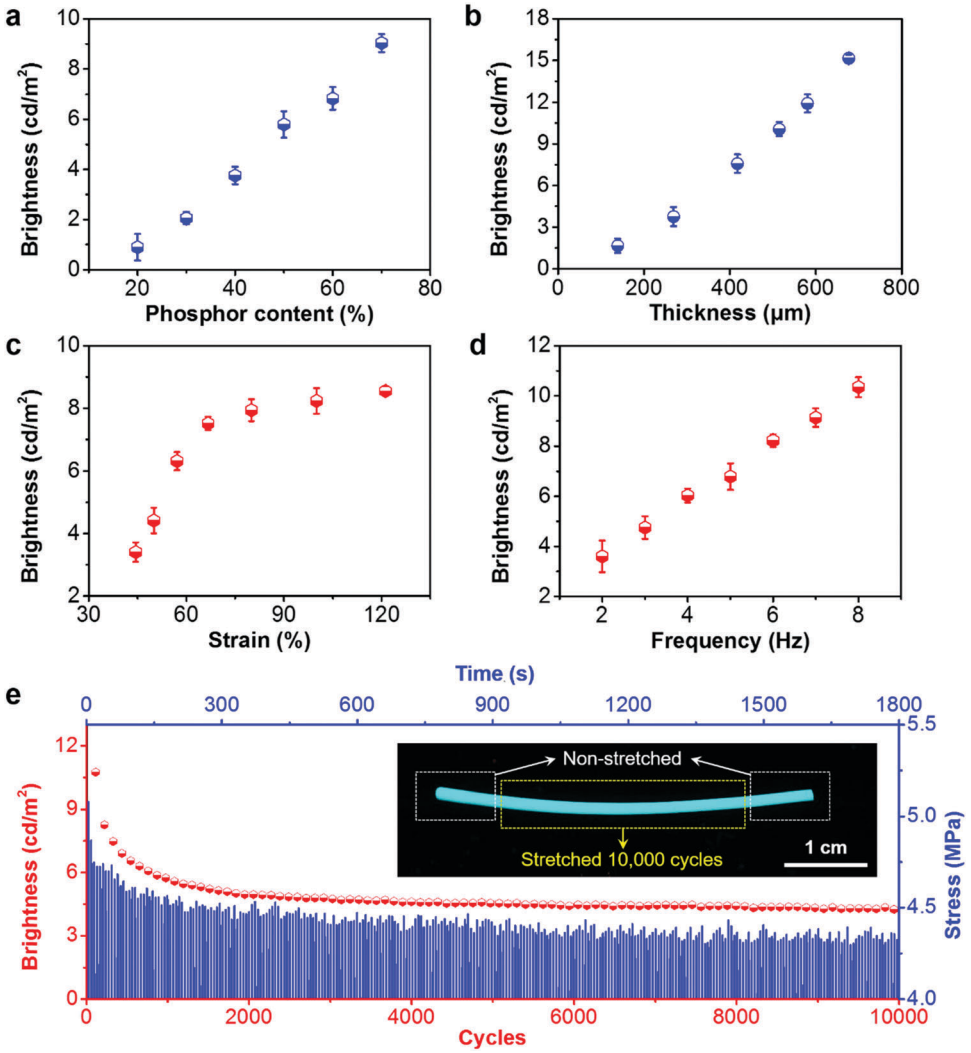

Fig. 2 Mechanoluminescence measurements. Dependence of the mechanoluminescence intensity of the composite fiber on phosphor content (a), thickness of the mechanoluminescent layer (b), strain (c) and frequency (d); (e) evolution of the mechanoluminescence intensity (red) and mechanical strength (blue) of the composite fiber during stretch and release cycles (inset, photograph of the composite fiber under UV irradiation after 10 000 cycles of stretch and release).

consistent with that of the mechanoluminescence intensity, indicating that the degradation of mechanoluminescence intensity may result from the creep and relaxation behavior of PDMS. Thus, a mechanoluminescent composite fiber with higher performance can be obtained by incorporating other elastic materials with better mechanical properties.

Traditional fabrics show a variety of colors based on diverse pigments. To further expand the applications of the mechanoluminescent fiber, mechanoluminescent fibers with different colors were also developed by mixing two ZnS phosphors with different colors. In addition to the ZnS:Cu phosphor, which emits green light, the ZnS:Mn phosphor, which displays an orange color during the deformation process, was also used. Mechanoluminescent composite fibers with several colors were realized by adjusting the weight ratio of the two phosphors. As shown in Fig. 3a, the light color generated from the composite fiber changed from green to yellow, and then to orange as the proportion of ZnS:Mn particles increased. To visualize the mixed color, the corresponding CIE (Commission Internationale de L'Eclairage) coordinates were determined for each composite fiber. In Fig. 3b, it can be seen that the color changed linearly from green (0.22, 0.56) to yellow (0.41, 0.51) and to orange (0.53, 0.44) as the weight ratio of ZnS : Mn particles increased. Although every individual fiber showed a uniform color to the naked eye, the color was in fact a secondary color. In the spectra shown in Fig. 3c, two obvious bands at 476.5 and 593.2 nm were observed, ascribed to the green-colored ZnS:Cu phosphor and to the orange-colored ZnS:Mn phosphor, respectively, which explains the color changes from green to orange. Therefore, the secondary color actually resulted from a mixture of two lights. The color regulation was a result of different numbers of green and orange emission spots, each of which corresponded to a single ZnS particle in the mechanoluminescent layer (Fig. 3d–f and Fig. S8, ESI†).

Besides the monochromatic mechanoluminescent composite fiber, a single composite fiber with several colors was also fabricated by simultaneously depositing various mechanoluminescent materials with different colors along the axial direction of the fiber. Fig. 3g and Fig. S9a (ESI†) show a bicolored fiber with green and orange colors arranged in an alternate fashion by mechanoluminescent and photoluminescent mechanism, respectively. Herein the CIE coordinates obtained from photoluminescence were different from those obtained from the mechanoluminescence due to different intensities and mechanisms, as shown in Fig. S10 (ESI†). Tricolored composite fibers were also fabricated by the same strategy (Fig. 3h and Fig. S9b, ESI†), in which the yellow mechanoluminescent material was composed of a mixture of green and orange phosphors. The multicolored fibers with distinct colors were a result of clear interfaces between two mechanoluminescent materials (Fig. 3i, j and Fig. S11, ESI†).

Generally, the mechanoluminescent fibers with unique one-dimensional structures showed stable mechanical and luminescent performances, which enabled us to directly weave them into fabrics (Fig. 4a). In addition, we also developed two other mechanoluminescent fabrics based on mechanoluminescent ribbons and dots deposited on the fabric substrates.

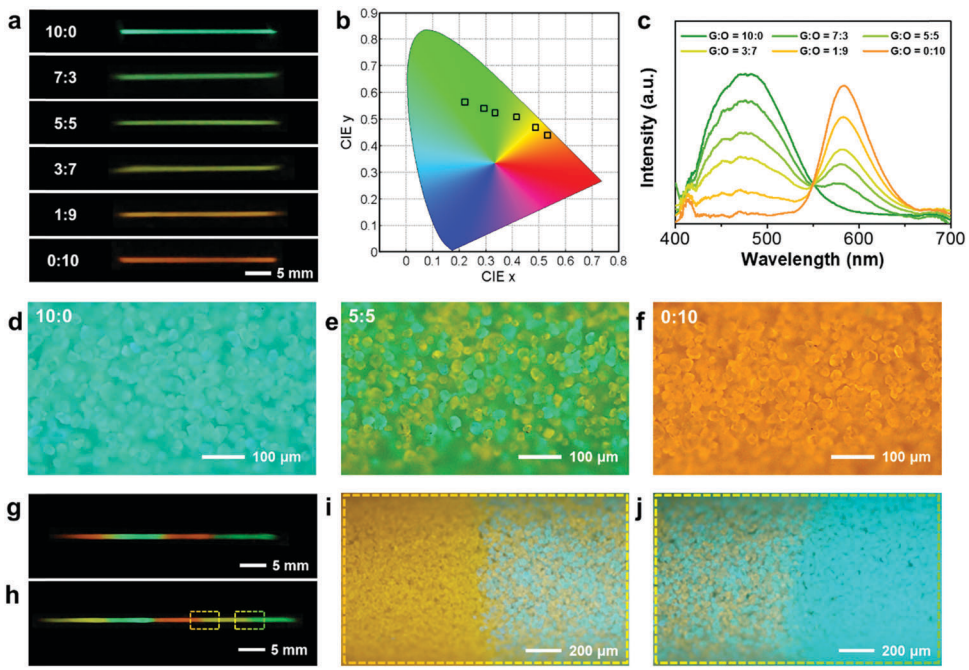

Fig. 3 Optical characteristics of the mechanoluminescent fibers. (a) Photographs of the mechanoluminescent fibers containing green and orange ZnS particles at weight ratios (green : orange) of 10 : 0, 7 : 3, 5 : 5, 3 : 7, 1 : 9 and 0 : 10; (b) and (c) CIE coordinates and luminescence spectra, respectively, of the mechanoluminescent fibers shown in (a); (d–f) optical microscope images of the mechanoluminescent fibers containing green and orange ZnS particles at weight ratios (green : orange) of 10 : 0, 5 : 5 and 0 : 10, respectively; (g) and (h) photographs of bicolored and tricolored mechanoluminescent fibers, respectively, during stretching; (i) and (j) optical microscope images of the interface between the orange and yellow lights, and the yellow and blue lights, respectively, in the composite fibers shown in (h).

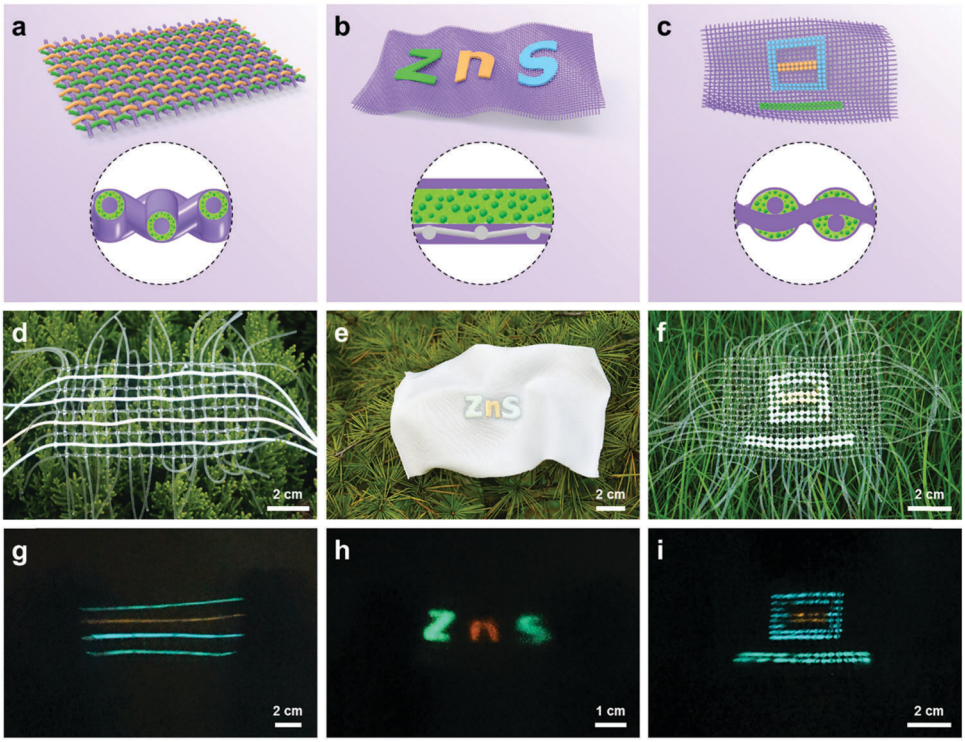

Fig. 4 Mechanoluminescent fabrics. Schematic illustrations with the structure of the mechanoluminescent fabrics based on mechanoluminescent fibers (a), ribbons (b) and dots (c); (d–f) photographs of the mechanoluminescent fabrics based on mechanoluminescent fibers (d), ribbons (e) and dots (f); (g–i) photographs of the mechanoluminescent fabrics shown in (d–f) during the stretch and release process.

The first strategy, which is the most accessible, consisted in directly depositing the mechanoluminescent materials onto the common elastic PDMS-coated fabric substrate to form a mechanoluminescent ribbon. As shown in Fig. 4b, the mechanoluminescent active materials with different colors were deposited successively onto a polyurethane cloth using a ZnS patterned mask. The structure and morphology of the fabrics during the preparation process are shown in Fig. S12 (ESI†). Alternatively, we could also design colorful patterns by selectively depositing a series of mechanoluminescent dots onto the intersections of an elastic fabric (Fig. 4c). These luminescent dots are just like pixels and therefore, more complex patterns with higher resolution can be designed by controlling the fabric network of coated sites. Although these strategies led to different designs, both fabrics presented a multi-layered structure similar to the mechanoluminescent fiber comprised of an inner substrate, a mechanoluminescent interlayer and an outer PDMS coating layer (Fig. S13, ESI†). The fabricated mechanoluminescent fabrics (Fig. 4d–f) could also emit colored light upon deformation such as stretching (Fig. 4g–i). Thus, these mechanoluminescent fabrics have potential applications in smart displays and fashionable ornaments, particularly for night illumination.

In summary, a novel mechanoluminescent fiber with a core–sheath structure able to emit a soft and tunable light was fabricated. The color of the mechanoluminescent fibers could be easily adjusted to display various monochromes, *e.g.*, green, orange or yellow. In addition, multicolored fibers, including bicolored and tricolored, were also realized in a single fiber. The mechanoluminescence intensity was well retained even after 10 000 cycles of stretch and release. Furthermore, mechanoluminescent fabrics were fabricated by weaving the composite fibers into a fabric or by directly depositing the mechanoluminescent active materials onto fabric substrates. The resulting mechanoluminescent fabrics exhibited promising characteristics and could find applications as flexible displays for fashionable ornaments and night illumination.

Acknowledgements

This study was supported by the MOST (2016YFA0203302), the NSFC (21634003, 51573027, 51403038, 51673043) and the STCSM (17QA1400400, 16JC1400702, 15XD1500400, 15JC1490200).

Notes and references

1 L. Liu, Y. Yu, C. Yan, K. Li and Z. Zheng, *Nat. Commun.*, 2015, **6**, 7260.
2 Y. C. Lai, B. W. Ye, C. F. Lu, C. T. Chen, M. H. Jao, W. F. Su, W. Y. Hung, T. Y. Lin and Y. F. Chen, *Adv. Funct. Mater.*, 2016, **26**, 1286.
3 X. Sun, J. Zhang, X. Lu, X. Fang and H. Peng, *Angew. Chem., Int. Ed.*, 2015, **54**, 3630.
4 J. Kim, A. Banks, Z. Xie, S. Y. Heo, P. Gutruf, J. W. Lee, S. Xu, K.-I. Jang, F. Liu, G. Brown, J. Choi, J. H. Kim, X. Feng, Y. Huang, U. Paik and J. A. Rogers, *Adv. Funct. Mater.*, 2015, **25**, 4761.

5 S. Takamatsu, T. Lonjaret, E. Ismailova, A. Masuda, T. Itoh and G. G. Malliaras, *Adv. Mater.*, 2016, **28**, 4485.
6 Z. Zhang, Y. Zhang, Y. Li and H. Peng, *Acta Polym. Sin.*, 2016, **10**, 1284.
7 J. J. Liang, L. Li, X. F. Niu, Z. B. Yu and Q. B. Pei, *Nat. Photonics*, 2013, **7**, 817.
8 A. Asadpoordarvish, A. Sandstrom, C. Larsen, R. Bollstrom, M. Toivakka, R. Osterbacka and L. Edman, *Adv. Funct. Mater.*, 2015, **25**, 3238.
9 M. K. Choi, J. Yang, K. Kang, D. C. Kim, C. Choi, C. Park, S. J. Kim, S. I. Chae, T. H. Kim, J. H. Kim, T. Hyeon and D. H. Kim, *Nat. Commun.*, 2015, **6**, 8.
10 R. H. Kim, M. H. Bae, D. G. Kim, H. Y. Cheng, B. H. Kim, D. H. Kim, M. Li, J. Wu, F. Du, H. S. Kim, S. Kim, D. Estrada, S. W. Hong, Y. G. Huang, E. Pop and J. A. Rogers, *Nano Lett.*, 2011, **11**, 3881.
11 W. S. Choi, W. J. Kim, S. H. Park, S. O. Cho, J. K. Lee, J. B. Park, J. S. Ha, T. H. Chung and T. Jeong, *Solid-State Electron.*, 2017, **127**, 57.
12 Z. Zhang, X. Shi, H. Lou, Y. Xu, J. Zhang, Y. Li, X.-L. Cheng and H. Peng, *J. Mater. Chem. C*, 2017, **5**, 4139.
13 M. D. Calisir, M. Erol, A. Kilic and H. Avci, *Dyes Pigm.*, 2016, **125**, 95.
14 S. Reineke, F. Lindner, G. Schwartz, N. Seidler, K. Walzer, B. Lussem and K. Leo, *Nature*, 2009, **459**, 234.
15 X. L. Dai, Z. X. Zhang, Y. Z. Jin, Y. Niu, H. J. Cao, X. Y. Liang, L. W. Chen, J. P. Wang and X. G. Peng, *Nature*, 2014, **515**, 96.
16 S. G. R. Bade, J. Q. Li, X. Shan, Y. C. Ling, Y. Tian, T. Dilbeck, T. Besara, T. Geske, H. W. Gao, B. W. Ma, K. Hanson, T. Siegrist, C. Y. Xu and Z. B. Yu, *ACS Nano*, 2016, **10**, 1795.
17 S. I. Park, Y. J. Xiong, R. H. Kim, P. Elvikis, M. Meitl, D. H. Kim, J. Wu, J. Yoon, C. J. Yu, Z. J. Liu, Y. G. Huang, K. Hwang, P. Ferreira, X. L. Li, K. Choquette and J. A. Rogers, *Science*, 2009, **325**, 977.
18 H. Sun, Y. Zhang, J. Zhang, X. Sun and H. Peng, *Nat. Rev. Mater.*, 2017, **2**, 17023.
19 J. Deng, Y. Zhang, Y. Zhao, P. N. Chen, X. L. Cheng and H. S. Peng, *Angew. Chem., Int. Ed.*, 2015, **54**, 15419.
20 Z. T. Zhang, X. L. Chen, P. N. Chen, G. Z. Guan, L. B. Qiu, H. J. Lin, Z. B. Yang, W. Y. Bai, Y. F. Luo and H. S. Peng, *Adv. Mater.*, 2014, **26**, 466.
21 W. Zeng, L. Shu, Q. Li, S. Chen, F. Wang and X. M. Tao, *Adv. Mater.*, 2014, **26**, 5310.
22 J. Ren, Y. Zhang, W. Y. Bai, X. L. Chen, Z. T. Zhang, X. Fang, W. Weng, Y. G. Wang and H. S. Peng, *Angew. Chem., Int. Ed.*, 2014, **53**, 7864.
23 Z. B. Yang, J. Deng, X. M. Sun, H. P. Li and H. S. Peng, *Adv. Mater.*, 2014, **26**, 2643.
24 H. Yang, C. R. Lightner and L. Dong, *ACS Nano*, 2011, **6**, 622.
25 Z. T. Zhang, K. P. Guo, Y. M. Li, X. Y. Li, G. Z. Guan, H. P. Li, Y. F. Luo, F. Y. Zhao, Q. Zhang, B. Wei, Q. B. Pei and H. S. Peng, *Nat. Photonics*, 2015, **9**, 233.
26 Z. T. Zhang, Q. Zhang, K. P. Guo, Y. M. Li, X. Y. Li, L. Wang, Y. F. Luo, H. P. Li, Y. Zhang, G. Z. Guan, B. Wei, X. R. Zhu and H. S. Peng, *J. Mater. Chem. C*, 2015, **3**, 5621.
27 Y. H. Kim, H. Cho, J. H. Heo, T. S. Kim, N. Myoung, C. L. Lee, S. H. Im and T. W. Lee, *Adv. Mater.*, 2015, **27**, 1248.
28 B. P. Chandra, V. K. Chandra and P. Jha, *Appl. Phys. Lett.*, 2014, **104**, 031102.
29 V. K. Chandra, B. P. Chandra and P. Jha, *Appl. Phys. Lett.*, 2013, **102**, 241105.
30 S. M. Jeong, S. Song, K. I. Joo, J. Kim, S. H. Hwang, J. Jeong and H. Kim, *Energy Environ. Sci.*, 2014, **7**, 3338.
31 S. M. Jeong, S. Song, S. K. Lee and N. Y. Ha, *Adv. Mater.*, 2013, **25**, 6194.
32 S. M. Jeong, S. Song, S. K. Lee and B. Choi, *Appl. Phys. Lett.*, 2013, **102**, 5.
33 D. O. Olawale, K. Kliewer, A. Okoye, T. Dickens, M. J. Uddin and O. I. Okoli, *Struct. Health Monit.*, 2014, **13**, 177.
34 C. Ralph, M. Silberstein, P. R. Thakre and R. Singh, *Mechanics of Composite and Multi-functional Materials*, Springer International Publishing, Switzerland, 2016, ch. 7, vol. 7, p. 63.
35 V. K. Chandra, B. P. Chandra and P. Jha, *Appl. Phys. Lett.*, 2013, **103**, 5.
36 B. P. Chandra, V. K. Chandra and P. Jha, *Physica B*, 2015, **461**, 38.
37 X. Y. Wei, X. D. Wang, S. Y. Kuang, L. Su, H. Y. Li, Y. Wang, C. F. Pan, Z. L. Wang and G. Zhu, *Adv. Mater.*, 2016, **28**, 6656.
38 K. S. Sohn, S. Timilsina, S. P. Singh, T. Choi and J. S. Kim, *APL Mater.*, 2016, **4**, 7.

